

C. Hellesen, M. Albergante, E. Andersson Sundén, L. Ballabio, S. Conroy, G. Ericsson,  
M. Gatu Johnsson, L. Giacomelli, G. Gorini, A. Hjalmarsson, I. Jenkins, J. Källne,  
E. Ronchi, H. Sjöstrand, M. Tardocchi, I. Voitsekhovitch, M. Weiszflog  
and JET EFDA contributors

# Neutron Spectroscopy Measurements and Modeling of Neutral Beam Heating Fast Ion Dynamics

“This document is intended for publication in the open literature. It is made available on the understanding that it may not be further circulated and extracts or references may not be published prior to publication of the original when applicable, or without the consent of the Publications Officer, EFDA, Culham Science Centre, Abingdon, Oxon, OX14 3DB, UK.”

“Enquiries about Copyright and reproduction should be addressed to the Publications Officer, EFDA, Culham Science Centre, Abingdon, Oxon, OX14 3DB, UK.”

The contents of this preprint and all other JET EFDA Preprints and Conference Papers are available to view online free at [www.iop.org/Jet](http://www.iop.org/Jet). This site has full search facilities and e-mail alert options. The diagrams contained within the PDFs on this site are hyperlinked from the year 1996 onwards.

# Neutron Spectroscopy Measurements and Modeling of Neutral Beam Heating Fast Ion Dynamics

C. Hellesen<sup>1</sup>, M. Albergante<sup>2</sup>, E. Andersson Sundén<sup>1</sup>, L. Ballabio<sup>3</sup>, S. Conroy<sup>1</sup>, G. Ericsson<sup>1</sup>,  
M. Gatu Johnsson<sup>1</sup>, L. Giacomelli<sup>4</sup>, G. Gorini<sup>3</sup>, A. Hjalmarsson<sup>1</sup>, I. Jenkins<sup>5</sup>, J. Källne<sup>1</sup>,  
E. Ronchi<sup>1</sup>, H. Sjöstrand<sup>1</sup>, M. Tardocchi<sup>3</sup>, I. Voitsekhovitch<sup>5</sup>, M. Weiszflog<sup>1</sup>  
and JET EFDA contributors\*

*JET-EFDA, Culham Science Centre, OX14 3DB, Abingdon, UK*

<sup>1</sup>*EURATOM-VR, Department of Physics and Astronomy, Uppsala University, SE-75120 Uppsala, Sweden*

<sup>2</sup>*EURATOM-Confédération Suisse, Ecole Polytechnique Fédérale de Lausanne (EPFL),  
CRPP, CH-1015 Lausanne, Switzerland*

<sup>3</sup>*EURATOM-ENEA sulla Fusione, IFP Milano, Italy*

<sup>4</sup>*PTB, Braunschweig, Germany*

<sup>5</sup>*EURATOM-CCFE Fusion Association, Culham Science Centre, OX14 3DB, Abingdon, OXON, UK*

\* See annex of F. Romanelli et al, "Overview of JET Results",  
(Proc. 22<sup>nd</sup> IAEA Fusion Energy Conference, Geneva, Switzerland (2008)).



## ABSTRACT

The energy spectrum of the neutron emission from beam-target reactions in fusion plasmas at the Joint European Torus (JET) has been investigated. Different beam energies as well as injection angles were used. Both measurements and simulations of the energy spectrum were done. The measurements were made with the time-of-flight spectrometer TOFOR. Simulations of the neutron spectrum were based on first principle calculations of neutral beam deposition profiles and the fast ion slowing down in the plasma using the code NUBEAM, which is a module of the TRANSP package. The shape of the neutron energy spectrum was seen to vary significantly depending on the energy of the beams as well as the injection angle and the deposition profile in the plasma. Cross validations of the measured and modeled neutron energy spectra were made, showing a good agreement for all investigated scenarios.

## 1. INTRODUCTION

In fusion plasmas, neutrons are produced in the nuclear reactions  $d(d,n)^3\text{He}$  (DD) and  $d(t,n)^4\text{He}$  (DT). Since the neutron emission from fusion plasmas is closely linked to the velocities of the reactants, neutron measurements can provide a variety of information about the motional state of the fuel ions. A robust method for validating plasma-modeling codes is to compare simulated synthetic diagnostics with measured data. In such case, the diagnostic need not measure a physical plasma parameter. E.g., when validating TRANSP [1] simulations, it is common to calculate the expected total neutron emission rates from the modeled plasma and compare with the measured rates [2]. The total neutron emission rate is sensitive to a large number of plasma parameters and traditionally a good match between model and measurement is considered a good benchmark of the simulations. Additional information can also be found in the energy spectrum of the neutron emission, where different parts of the fuel ion population reveal themselves through certain signatures, reflecting the kinematics of the fusion reactions. For examples, fusion plasma in thermal equilibrium gives a neutron energy spectrum of nearly Gaussian shape, while anisotropic ion populations resulting from external heating, are characterized by different shapes depending on the type of heating.

In this paper, the detailed properties of the neutron emission spectrum from beamplasma reactions due to Neutral Beam Injection (NBI) at the Joint European Torus (JET) [3] are studied. Both modeling of the neutron energy spectra, including the full geometry of the spectrometers sight line, as well as experimental measurements were made. The modeling is based on first-principle calculations of the slowing-down distribution of the beam ions and was calculated with the code NUBEAM [4], which is a module of the TRANSP package. NUBEAM computes time-dependent deposition profiles and slowing down of the fast ions produced by NBI, taking into consideration, among other effects, beam geometry, large scale instabilities such as sawteeth and finite-Larmor radius effects. Using the modeled slowing-down distribution, the volume integrated neutron emission spectrum was calculated with the Monte Carlo code ControlRoom [5]. The results were compared with spectroscopic measurements of the plasmas using the neutron time of flight spectrometer TOFOR

[6]. Neutral beams with different energies and injection angles were studied. It was found that both the energies of the beams and their injection angles had great importance on the shapes of the resulting neutron emission spectra.

## 2. FUSION NEUTRON EMISSION SPECTRA

In nuclear fusion research, there are two neutron-producing fusion reactions that are widely studied, namely  $d(d,n)^3\text{He}$  and  $t(d,n)\alpha$ ; these are hereafter referred to as DD and DT reactions, respectively. The energy of the emitted neutron,  $E_n$ , carries information on the velocities of the reactants involved [7] and is given by:

$$E_n = \frac{1}{2} m_n v_{\text{cm}}^2 + \frac{m_R}{m_n + m_R} (Q + K) + v_{\text{cm}} \cos(\theta) \left( \frac{2m_n m_R}{m_n + m_R} (Q + K) \right)^{1/2}, \quad (1)$$

where

$$K = \frac{1}{2} \mu v_{\text{rel}}^2 \quad \text{and} \quad v_{\text{cm}} = \frac{m_1 v_1 + m_2 v_2}{m_1 + m_2}. \quad (2)$$

$Q$  is the total energy released in the nuclear reaction, which is 3.27 MeV in the case of DD fusion and 17.6 MeV in DT fusion.  $K$  is the reactants relative kinetic energy and  $\mu$  is their reduced mass;  $m_R$  denotes the mass of the residual nucleus,  $m_n$  the neutron mass and  $\theta$  is the angle between the relative velocity of the reactants and the emission of the neutron in the centre of mass frame. To calculate the neutron energy spectrum from the interactions of two ion distributions,  $f_1$  and  $f_2$ , one needs to calculate the integral

$$\frac{dN}{dE} = \frac{1}{4\pi} \int_{\vec{v}_1} \int_{\vec{v}_2} f_1(\vec{v}_1) f_2(\vec{v}_2) \delta(E - E_n) v_{\text{rel}} \sigma(v_{\text{rel}}, \theta) dv_1 dv_2. \quad (3)$$

In this paper we focus on the neutron emission spectrum from beam-plasma DD reactions. To understand the properties of this spectrum, consider a beam with energy  $E_{\text{beam}}$  interacting with a thermal background plasma, i.e.  $E_{\text{beam}} \gg E_{\text{th}}$ . At JET, where the energy of the beams are around 100 keV, the released fusion energy of beamplasma reactions is much larger than the kinetic energy of the reactants, i.e.,  $K \ll Q$ . Given these two conditions, the first term in Eq. (1) will be negligible, the second term will be nearly constant and the third term will be proportional to  $v_{\text{cm}} \cos(\theta)$ . If the spectrum is measured in a direction perpendicular to the  $B$  field, the cyclotron motion of the beam ions will make  $\cos(\theta)$  vary roughly between  $\pm v_{\perp}/v$ . The emission spectrum will thus be centered at about 2.5 MeV and, due to the cyclotron motion of the ions, have a width proportional to  $\sqrt{E_{\text{beam}}}$ . Furthermore, the width of the spectrum will also be proportional to the ratio of the perpendicular velocity component to the total velocity, i.e.,  $v_{\perp}/v$ .

### 3. EXPERIMENTAL

To achieve the best conditions to investigate the neutron emission spectrum from NBI heating, low temperature plasmas where the neutron emission is dominated by beam plasma reactions were examined. These conditions give rise to the sharpest features in the neutron energy spectrum and provide the most sensitive tests of the model assumptions. Two low power JET discharges, namely Pulse No's: 69242 and 68138, were suitable for this study.

Pulse No: 69242 was heated with a series of NBI blips of 2 s each. The NBI blips used a single Positive Ion Neutral Injector (PINI) module each. This gave the opportunity to study the plasma response to different NBI configurations, both in terms of injection energy ( $E_{\text{beam}}$ ) and direction of injection, on or off axis as well as normal or tangential with respect to the magnetic field. Three time periods at 15.5-17.5, 18.0-20.0 and 20.5-22.5 seconds were analyzed for Pulse No's: 69242. These are hereafter referred to as periods I, II and III, respectively.

In contrast, Pulse No's: 68138 was heated for 8 s with a single NBI PINI. The long steady-state duration of the NB heating phase provided ample time to collect data with good statistics despite the modest heating power. This allowed for a detailed shape comparison of the modeled and the measured data.

The detailed setup of the NBI heating systems are given in Table 1 and the projection of the trajectories on the poloidal plane, for the relevant PINIs, are shown in Figure 1. Note that the use of normal and tangential is a nomenclature for the alignment of the NBI PINIs. Normal refers to trajectories that hit the central column, making a single pass through the plasma (4.3, 8.3 and 8.6 in Figure 1) and tangential refers to trajectories that make a double pass through the plasma (4.1 in Figure 1). The actual injection angle with respect to the magnetic field is about 60 degrees for both types of alignment.

The energy spectrum of the neutron emission was measured with the TOFOR (Time Of Flight Optimized for Rate) neutron spectrometer. TOFOR is installed in the roof laboratory at JET and views the center of the plasma with a vertical viewing cone (Figure 1) at a distance of about 19 m. The neutron time-of-flight ( $t_{\text{TOF}}$ ) is obtained from the time difference between interactions in two sets of detectors: 5 primary detectors and 32 secondary detectors. The distance between the primary and the secondary detectors in TOFOR is 1.2m, which to 1st order results in a  $t_{\text{TOF}}$  of about 65ns for neutrons with  $E_n = 2.5\text{MeV}$  from DD fusion reactions. The detailed shape of the response function of TOFOR, i.e. the mapping from  $En$  to  $t_{\text{TOF}}$  is simulated to high precision with a full Monte Carlo model of the spectrometer for neutron energies from 1 to 7MeV [8]. Having the full response function, it is possible to fold a calculated neutron energy spectrum with the response function. This allows for a direct comparison of the predicted neutron energy spectra and measured data on a  $t_{\text{TOF}}$  scale.

TRANSP simulations were made for the two discharges studied. In TRANSP, the code NUBEAM is used to calculate the deposition profile and slowing down of the beams in the plasma. NUBEAM calculates the beam-ion slowing-down distribution ( $f_{\text{NBI}}$ ) in four dimensions: poloidal space

coordinates ( $\theta$  and  $\rho$ ) as well as energy and pitch angle ( $E_d$  and  $\xi$ ), where the pitch-angle is given as the ratio of the velocity component parallel to the magnetic field and the magnitude of the velocity  $\xi = v_{\parallel}/v$ . The ion orbits are averaged over the gyro motion and toroidal symmetry is assumed. In Figure 2, the simulated beam deposition profile is shown versus the normalized poloidal flux for the on-axis 127keV beam from period II and the off-axis 115 keV beam from period III in Pulse No: 69242.

The volume-averaged  $f_{\text{NBI}}$  for these two beams are shown in Figure 3. Both the beam deposition profiles as well as the pitch angle distributions for the two beams are undoubtedly different. For the on-axis beam,  $\alpha$  is concentrated to a narrow band from 0.5 to 0.8, while for the off-axis beam;  $\alpha$  is spread in a wide band from  $-0.5$  to  $0.7$ .

Using the simulated  $f_{\text{NBI}}$  and estimates of the background plasma profile ( $n_i$  and  $T_i$ ), the expected neutron energy spectra were calculated using Eq. (1) and (3) with the code ControlRoom. The geometry of the TOFOR viewing cone was used to integrate Eq. (3) over the emitting plasma volume.

The modeled neutron energy spectra for the time periods I, II and III of discharge JET Pulse No: 69242 are shown in Fig.2. The double-humped shapes of the spectra are typical of that from a distribution of fast ions interacting with cold background plasma. The full width at half maximum (FWHM) of the spectra are given in Table 2.

TOFOR data were extracted for the 8 s duration of the NBI heating phase of Pulse No: 68138 and from the three time periods of JET Pulse No: 69242. In the former discharge, the total neutron emissivity rates ( $R_{\text{NT}}$ ) were  $2.3 \times 10^{14} \text{ s}^{-1}$  and in the latter,  $R_{\text{NT}}$  was  $1.0 \times 10^{14} \text{ s}^{-1}$ ,  $2.6 \times 10^{14} \text{ s}^{-1}$  and  $1.5 \times 10^{14} \text{ s}^{-1}$  for periods I, II and III, respectively. The  $t_{\text{TOF}}$  spectrum from Pulse No: 68138 is shown in Figure 5a (data with errorbars). The total number of neutrons in the spectrum was 9200, corresponding to a count rate of 1050Hz. This provided good statistics to investigate the details in the spectral shape, which from 60 to 70ns is reminiscent of the modeled spectrum due to beam-target reactions that as discussed above (Figure 4), although with some resolution broadening. This part is mainly the result of direct scattering between the primary and the secondary detectors in TOFOR. The tail at  $t_{\text{TOF}} > 70$  ns on the other hand is due partly to multiple scattering within the spectrometer itself as well as to contributions from low energy neutrons that have scattered in the far wall of the JET vacuum vessel [9]. Both of these effects are included in the data analysis; the multiple scattering in the spectrometer is treated as a part of the instrumental response function and the scattering in the vessel is included as a separate spectral component. By folding the modeled neutron emission spectra with the TOFOR response function, thus obtaining a modeled  $t_{\text{TOF}}$  spectrum, a direct comparison between the modeled TRANSP results and the experimental TOFOR data can be made. The experimental  $t_{\text{TOF}}$  data were analyzed using a two-component model representing the NBI heating and its associated low-energy scattered emission as shown in Figure 5a (black dashed and red dash-dot, respectively) together with the summed total (solid blue). The twocomponent model was fitted to the experimental data and only the intensities of the components were left as



free parameters. The overall match is good, both in terms of spectral width and qualitative shape. The reduced  $\chi^2$  of the fit was 1.5.

While the 8-second steady state heating in Pulse No: 68138 allowed for a detailed examination of the shape of the spectrum, the three shorter time periods in Pulse No: 69242 provided data with lower statistics. The count rates in TOFOR were 340Hz, 1240Hz and 480Hz for periods I, II and III respectively. Measured  $t_{\text{TOF}}$  data from periods I and III are shown in Figure 6 along with their corresponding modeled data, which were obtained as described above. Also for this discharge, good matches in the overall shapes between modeled and measured data are seen, with reduced  $\chi^2$  of 1.0 and 0.7.

Although it is harder to make as detailed comparisons as above due to the lower statistics, the Full Width at Half Maximum (FWHM) of the spectra is a robust parameter and comparisons between models and measurements are given in table 2. The FWHM of TOFOR data was obtained using the modeled spectra and stretching or compressing them until the optimal widths in terms of  $\chi^2$  were found. The uncertainties are estimated from an increase in  $\chi^2$  of 1 unit. The widths of the measured and the modeled data are seen to agree within the statistical uncertainties of the measurements with the exception of discharge 68138 where a slightly lower value of 1.5% is seen.

## 5. DISCUSSION

The agreement between the TRANSP/NUBEAM model and TOFOR measurements demonstrated in this paper relies on an approach where the full geometry of the spectrometer viewing cone as well as the complete beam-ion distribution function in 4 dimensions is employed. A potential source of error in this analysis could be the absence of thermo-nuclear and beam-beam emission. Measurements of ion temperatures, that are needed to calculate the thermo nuclear emission, were however not available for these discharges since no diagnostic beams were used. However, due to the low heating power, the central electron temperature did never exceed 2.5keV during the discharge. At such low electron temperature, the energy transfer from the beam-ions to the bulk-ions is small and the ion temperature is not expected to be larger than the electron temperature. Due to the low plasma temperature, the contribution from the thermo-nuclear neutron emission is estimated to less than 3% of the total emission. This is negligible and can safely be ignored for the purpose of the present analysis. The contribution from beam-beam neutron emission is also estimated to be very low at a few percent, which is a consequence of the low heating power and hence, low beam ion concentration.

As expected from Eq. (1), the spectrum from the beam with lowest energy, 77keV, is narrower than the those from the three beams of higher energy. However, of the three high-energy beams, the one with lowest energy (PINI 8.3) results in a significantly wider spectrum than that of highest energy (PINI 4.1), FWHM = 680keV compared with 630keV, respectively. At first sight, this result might seem counter intuitive. However, the width of the neutron spectrum is determined from the combination of  $E_d$  as well as  $\xi$ . As discussed above, higher  $v_{\perp}/v$ , i.e. lower  $\xi$ , results in wider neutron energy spectra. Thus, even though PINI 8.3 has lower injection energy compared with

PINI 4.1, the normal injection angle will result in ions with higher  $v_{\perp}$  (Figure 3), and hence result in a wider neutron spectrum. However, the difference in injection angles of about  $2\text{-}3^{\circ}$  is too small to fully account for the increased spectral width and does not explain the different results from PINI 8.3 and 8.6, which are both normal. The results can be fully understood from the properties of ion orbits in toroidal geometry. Due to conservation of magnetic moment, the evolution of  $\xi$  in the absence of pitch-angle scattering is given by

$$\xi = \frac{v_{\parallel}}{v} = \sqrt{1 - \frac{\Lambda R_0}{R}},$$

where  $\Lambda$  is a constant of motion for the ion,  $R_0$  is the major radius of the torus and  $R$  is the position of the particle along the major radius. The consequence is that when ions move towards lower  $R$ , the pitch angle decreases to conserve the particles magnetic moment. The minimum magnitude of the pitch angle,  $|\xi| = 0$ , is obtained at  $R = \Lambda R_0$ , where the ion velocity is purely perpendicular. This is called the turning point of trapped particle orbits. Here,  $v_{\parallel}$  changes sign and the ion is reflected back towards higher  $R$ . As shown in Figure 2, the deposition profile for on-axis beams is peaked in the center and for off-axis beams it is peaked at  $\rho \approx 0.4$ . Consequently, for on-axis injection, the ions can only undergo small excursions in  $R$ . Therefore,  $\xi$  is rather constant during slowing down. On the other hand, for off-axis injection, a  $\rho$  of 0.4 allows for a variation in  $R$  from 2.5 m to 3.3m. The consequence is a larger variation in  $\xi$  during slowing down, which explains the fundamentally different shapes of  $f_{\text{NBI}}$  (Figure 3) as well as the different widths of the spectra from PINI 8.3 and 8.6, with on-axis and off-axis alignment, respectively. The plasma scenarios analyzed in this paper are low-density plasmas, which allows for a deep penetration of the beams into the center of the plasma. On the contrary, in a high-density plasma the beam cannot penetrate as deep; consequently, also on-axis beam injection will result in a deposition profile peaked off-axis at larger minor radii. Therefore, the shape of the neutron energy spectrum from beam-plasma reactions is expected to vary between different plasma conditions.

Since the reactivity of the DD reaction rises by an order of magnitude from thermal plasma energies to the beam injection energy, the shape of the neutron emission spectrum is primarily decided by the properties of the high-energy part of the slowing down distribution. Therefore, it is also that part of the slowing down distribution that is tested with the analysis presented here.

Previous analysis of neutron emission spectroscopy data has discussed how different orbits (mainly trapped and passing) play an important role for the shape of the neutron energy spectrum [10]. The study presented here is however the first demonstration where the effect is quantified with first principle calculations (NUBEAM) and confirmed by measured data (TOFOR). These results are important in two ways.

First, they can be seen as a solid benchmark of the plasma modeling codes used, namely TRANSP and NUBEAM. The analysis allowed for detailed studies of e.g. orbit effects due to different types of beam injection; on or off axis as well as tangential and normal injection. The results found where

consistent with simulations, which can be seen as a good verification that the physics assumptions made in the codes are sound and accurately describes the beam ion properties that NES is most sensitive to. NES analysis could also be used in a similar fashion to benchmark other codes, e.g. PION [11], modeling radio frequency (RF) heating. A continuous validation of such codes is important since they are vital for the understanding of present day fusion experiments and the prediction of future ones.

Second, in fusion experiments aiming to approach burning plasma conditions, it is important to distinguish the thermonuclear fusion reactivity from the supra thermal due to external heating. In that case, several other components need to be used, representing, e.g., thermonuclear emission, beam-beam emission as well as that from supra-thermal ion-distributions due to RF heating. In such analyses, a good understanding of the shapes of the neutron energy spectra is crucial. Since the components partially overlap in energy their detailed shapes need to be well established in a spectroscopic analysis. If the components used in the analysis are not accurately modeled, systematic errors that are difficult to estimate will be introduced.

## CONCLUSIONS

Detailed modeling of fast ion distributions from neutral beam heated plasmas has been made using the TRANSP/NUBEAM codes. Volume integrated neutron emission spectra from the modeled ion distributions were calculated for the viewing cone of the TOFOR spectrometer. The detailed shape of the spectra was seen to be dependent on the injection energy as well as the injection angle and beam deposition profile. TOFOR measurements of the calculated neutron emission confirmed the modeling to unprecedented accuracy for neutron emission spectroscopy analysis.

## ACKNOWLEDGEMENTS

This work, supported by the European Communities under the contract of Association between EURATOM and VR, was carried out under the framework of the European Fusion Development Agreement. The views and opinions expressed herein do not necessarily reflect those of the European Commission

## REFERENCES

- [1]. Ongena, J. 1998, Transactions of Fusion Technology, Vol.33, p.181.
- [2]. Budny, R.V. 1995, Nuclear Fusion, Vol.35, p.1497.
- [3]. Rebut, P.M. and Keen, B.E. 1987, Fusion Technology, Vol.11, p.13.
- [4]. Pankin, A. 2004, Computer Physics Communications, Vol.159, p.157.
- [5]. Ballabio, L. *Control Room 0.3.7 User Manual*. 2008. Technical Manual.
- [6]. Gatu Johnsson, M. 2008, Nuclear Instruments Methods A, Vol.591, p.417.
- [7]. Brysk, H. 1973, Plasma Physics, Vol.15, p.611.
- [8]. Hjalmarsson, A. *Development and Construction of a 2.5MeV Neutron Time-of-Flight*

*Spectrometer Optimized for Rate (TOFOR)*. Department of Neutron Research. Uppsala : Uppsala University, 2006. PhD Thesis.

- [9]. Gatu Johnson, M. *The TOFOR Neutron Spectrometer For High Performance Measurements of D Plasma Fuel Ion Properties*. Varenna: AIP, 2007. Transactions of Buring Plasma Diagnostics.
- [10]. Henriksson, H. 2005, Plasma Physics and Controlled Fusion, Vol.47, p.1763.
- [11]. Mantsinen, M. 1999, Plasma Physics and Controlled Fusion, Vol.41, p.843.

JET Pulse No:	Time	NBI-PINI	$E_{\text{beam}}$ [keV]	alignment
69242	15.5 - 17.5	4.3	74	norm. off-axis
...	18 - 20	4.1	127	tang. on-axis
...	20.5 - 22.5	8.3	113	norm. off-axis
68138	17 - 25	8.6	116	norm. on-axis

Table 1: Setup of NBI heating systems for the two JET Pulse No's: 69242 and 68138.

NBI-PINI	Alignment	Energy	FWHM
4.3	off-axis norm	77 keV	540 keV
4.1	on-axis tang	127 keV	630 keV
8.3	on-axis norm	116 keV	660 keV
8.6	off-axis norm	113 keV	680 keV

Table 2: FWHM of modeled neutron spectra for different configurations of NBI heating.

NBI-PINI	TOFOR	TRANSP
off-axis norm. 77 keV	$7.8 \pm 0.3$ ns	7.9 ns
on-axis tang. 127 keV	$8.9 \pm 0.1$ ns	8.9 ns
on-axis norm. 116 keV	$9.55 \pm 0.07$ ns	9.41 ns
off-axis norm. 113 keV	$9.8 \pm 0.2$ ns	9.6 ns

Table 3: FWHM in ns of measured data (TOFOR) and modeled (TRANSP) spectra.

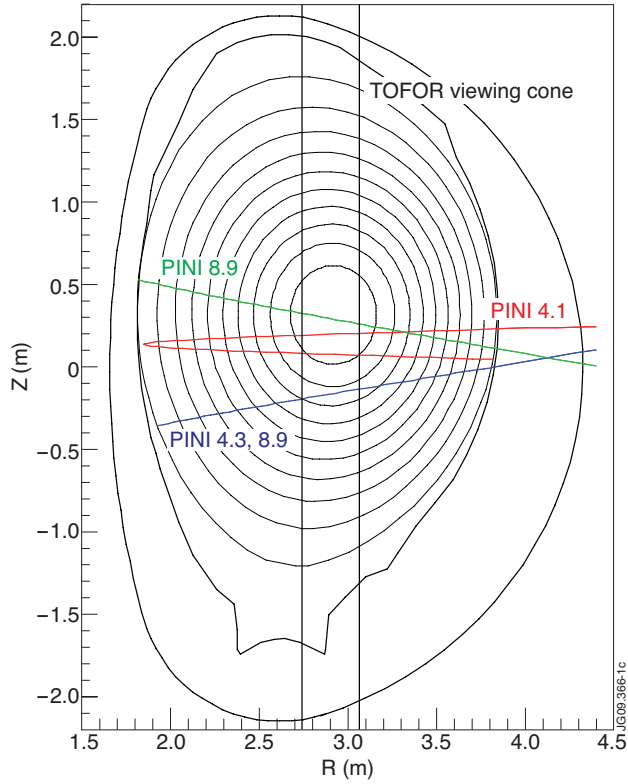


Figure 1: Poloidal cross section of the JET torus. The boundaries of the TOFOR viewing cone are illustrated as the vertical black lines. The trajectory of NBI PINI 4.1 is shown in red and those of 4.3+8.8 in blue and 8.6 in green.

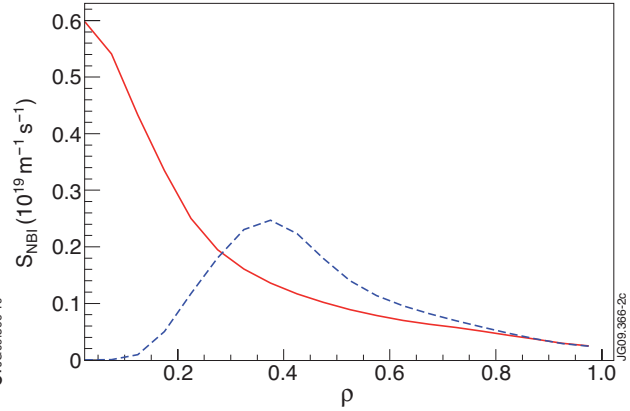


Figure 2: NBI deposition profile versus normalized poloidal flux for on-axis (red-solid) and off-axis (blue-broken).

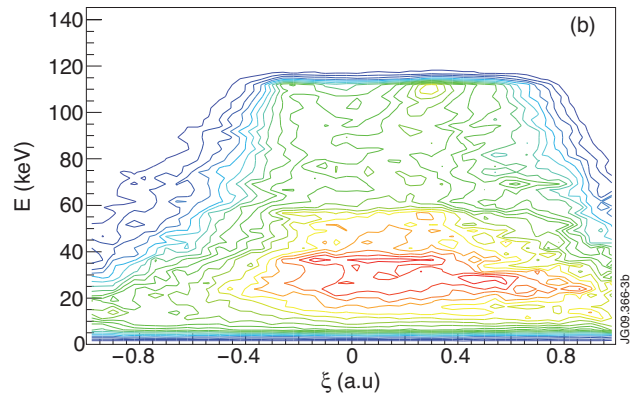
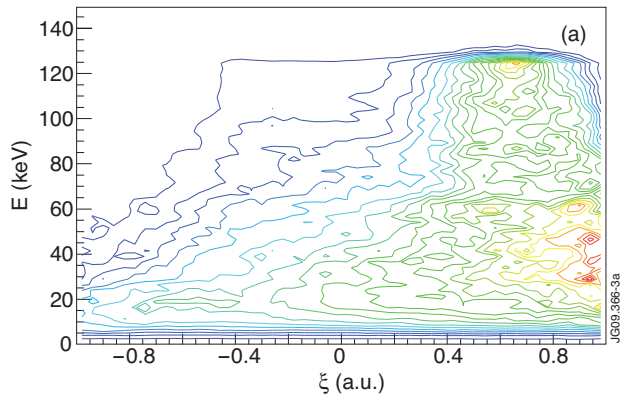


Figure 3: Calculated beam-ion slowing-down distribution ( $f_{NBI}$ ) for on-axis normal 127keV injection (a) and off-axis tangential 113keV injection (b).

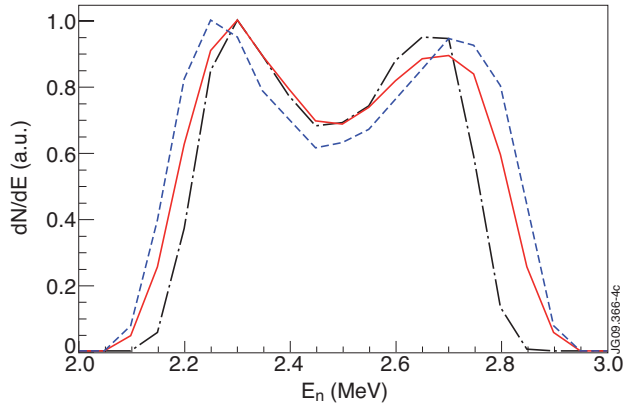


Figure 4: Calculated neutron spectra from the TRANSP ion distributions for 70keV off-axis (black broken-dot), 127keV on-axis (red solid) and 115keV off-axis (blue dashed).

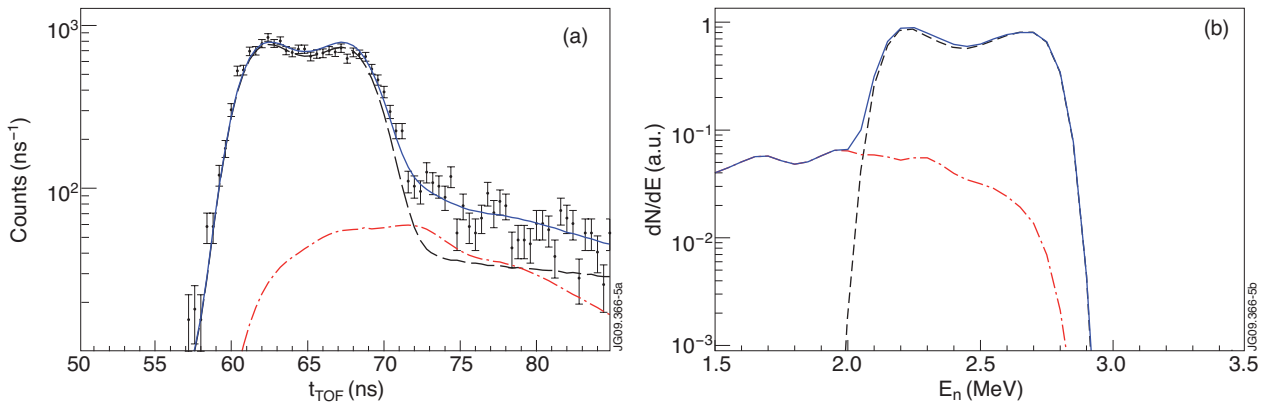


Figure 5: (a) TOFOR data from JET Pulse No: 68138 heated with 116keV NBI. Also shown is a fit of the calculated spectral components. (b) Energy representation of the fitted components, NBI (black dashed), backscatter (red dash-dot) and their sum (blue solid).

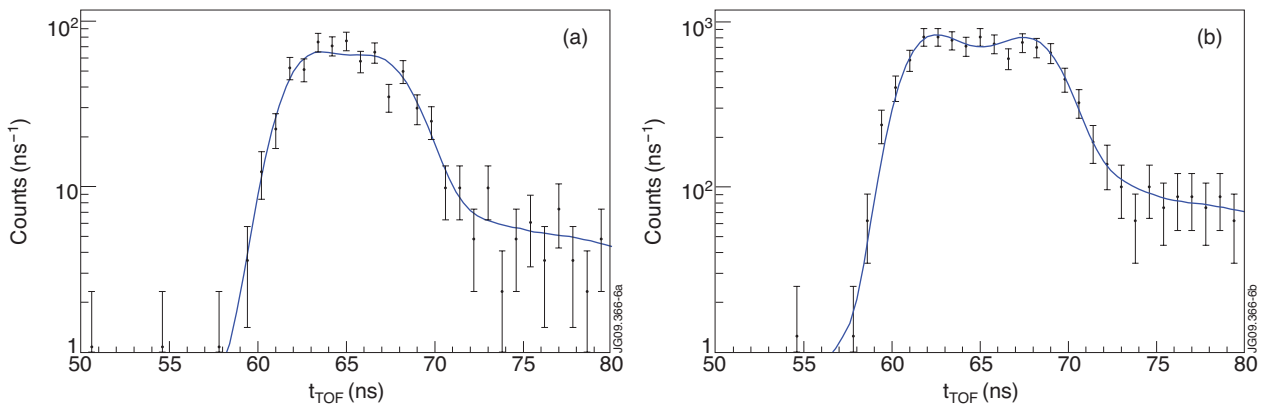


Figure 6: (a) TOFOR data from 77keV NBI heating during period I and (b) from 113keV NBI heating during period II of JET Pulse No: 69242. Also shown are the calculated neutron energy spectra (solid lines).